Available online at www.sciencedirect.com
ScienceDirect
Journal of Organometallic Chemistry 692 (2007) 225–233
Journal of Organometallic Chemistry
www.elsevier.com/locate/jorganchem

Automated design of protecting molecules for metal nanoparticles by combinatorial molecular simulations

Toshi Nagata *

National Institutes for Natural Sciences (NINS), Institute for Molecular Science (IMS), 5-1 Higashiyama, Myodaiji, Okazaki 444-8787, Japan
Department of Structural Molecular Science, Graduate University for Advanced Studies (Sokendai), 5-1 Higashiyama, Myodaiji, Okazaki 444-8787, Japan

Received 28 February 2006; received in revised form 5 May 2006; accepted 16 May 2006
Available online 30 August 2006

Abstract

New tripod oligo(dibenzyl sulfide) molecules were designed by computer modeling calculations so that they would form 1:1 complexes with an Au_{147} nanoparticle. Twelve aromatic molecules containing two methylthiomethyl groups were used as construction units (''residues''). Combinations of the residues (''sequences'') were examined by molecular dynamic simulations, and those sequences giving the largest interaction energies with the gold nanoparticle were sought through either full search or genetic algorithm. Best-fit sequences were found for $N = 5$ and 6 (N is the number of ''residues'' in one leg of the tripod molecule).

Keywords: Nanoparticle; Protection; Thioether; Molecular dynamics; Combinatorial computational chemistry; Genetic algorithm

1. Introduction

Recently metal nanoparticles have gained much interest [1] as useful materials in the fields of nanoscale electronics [2], photonics [3], as well as catalytic chemistry [4]. One particularly interesting area is the combination of metal nanoparticles with organic molecules that will lead to a new type of ''organometallic'' materials. The pioneering work of Brust et al. [5] opened the field of monolayer protected clusters (MPC) [6]. These materials exhibit excellent stability and have found numerous applications in various fields [7]. However, from a ''molecular'' point of view, these materials are complex mixtures of metal nanoparticles and indeterminate numbers of protecting molecules, and we often need to handle them as an ensemble of materials with a certain distribution of size and composition.

Such complexity may be resolved when we can make one-to-one composites of metal nanoparticles and protecting molecules. However, it is not easy to design protecting molecules that just ''fit'' the metal nanoparticles. The difficulty lies in the fact that we need to cover a spherical surface with a set of molecular fragments. This cannot be easily done by intuitive design.

Herein we propose an automated designing protocol of protecting molecules based on the concept of combinatorial computational chemistry [8]. The basic architecture of the target molecules is the same as in our previous study [9]; they are tripod molecules with an oligo(dibenzyl sulfide) framework (Fig. 1a). Between the sulfide linkage aromatic groups are placed, which are selected from those shown in Fig. 1b. We call these aromatic groups ''residues'', and the kinds and orders of the residues within one particular leg ''sequences'', by analogy with the peptide chemistry. Our aim is to find the best-fit sequences by calculations.

2. Computational methods

2.1. General

The atom types and force field parameters were taken from the parm99 force field distributed with AMBER 7 (all-atom version) [10]. Nonbonding interaction between the organic molecules and the gold nanoparticle was imple-

* Tel.: +81 564 59 5531; fax: +81 564 59 5510.
E-mail address: toshi-n@ims.ac.jp.

0022-328X/$ - see front matter © 2006 Elsevier B.V. All rights reserved.
doi:10.1016/j.jorganchem.2006.05.058

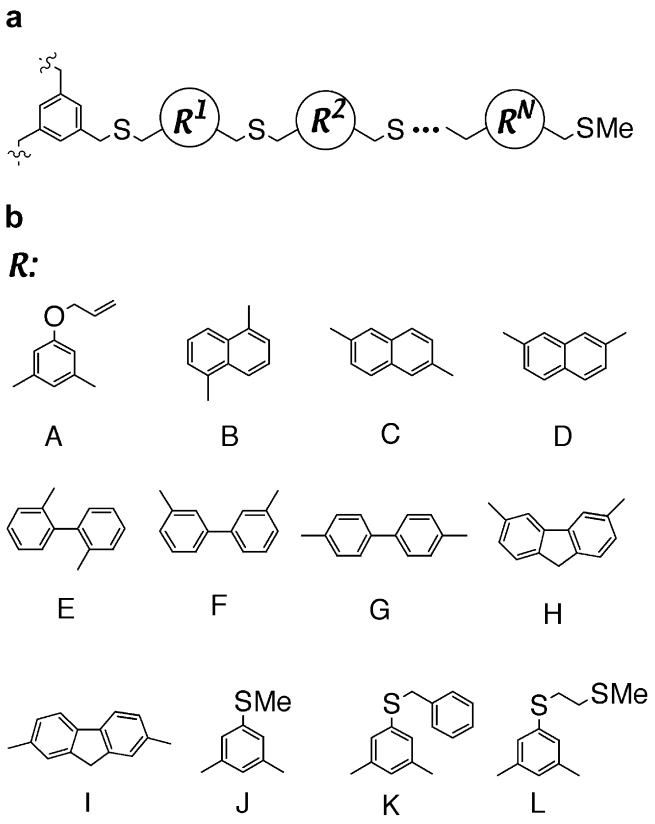

Fig. 1. (a) The base structure of the target molecule. (b) The "residues" used in this study.

mented as in our previous report [9]. The molecular dynamic (MD) calculations were performed mainly with a homemade program package named LWMD, although the NAMD program package [11] was also used (mainly for checking purposes). A timestep of 1 fs was used, with no constraints for hydrogen atoms. The temperature was maintained at 300 K by rescaling the velocities every 200 steps. Solvents were not included. We previously claimed that we needed to include the solvent to predict the solution structure of this type of molecules correctly [9]. However, in the present study we need to reduce the computational demand as much as possible, because we want to calculate a large number of combinations. The problem of simulations in a vacuum is the collapsing of the molecules by intramolecular van der Waals (vdW) interactions [12], but we can avoid this by cutting off the vdW terms at short distances. So we made the cutoff distances between the organic atoms at the equilibrium distance (i.e. the sum of vdW radii) for each pair of atoms. This is a crude approximation, but sufficient for screening purposes. Visualization of the structures were done with VMD [13]. Calculations were performed on a Silicon Graphics SGI2800 computer and a local cluster of Apple PowerMac G5 machines.

2.2. Preparation of residues

We defined each residue by appending two methylthiomethyl (CH_3SCH_2–) groups at appropriate positions of the aromatic molecule. A preliminary structure was built by use of the Chem3D program package (CambridgeSoft). The equilibrium structure and the RESP (restrained electrostatic potential fit) atomic charges [14] were obtained by quantum chemical calculation (HF/6-31G*) with GAMESS [15], followed by treatment with the RESP module of AMBER. The atomic coordinates and the RESP charges of the residues are given in Supporting information.

2.3. Automatic building of initial structures

We built a sequence from the component residues as shown in Fig. 2; namely, one methyl group and one methylthio (CH_3S–) group were formally removed to make an interresidue bond.

An obvious problem here is how to determine the relative geometry of the interconnecting two residues. One method is to fix the bond lengths and angles, and rotate the single bonds until all atom collisions are relieved. This is a useful technique in generating, for example, peptide structures. However, it is not suitable for the present application, because it tends to give random, unpredictable structures, whereas we want to restrict the initial structures so that we can quickly find the possible best-fit candidates. Although we might ultimately need to do a complete search over all structural space starting from random structures, it is too resource-demanding to be useful at the screening stage.

Instead, we placed the residues with our preferential orientations, and with sufficient interresidue distances to avoid any atom collisions. This naturally resulted in extremely long "bonds" between the residues, as illustrated in Fig. 2 with the bold lines. These "abnormal" bonds were relieved by short runs of molecular dynamic simulations with special treatments of the abnormal bonds as follows: (1) Find all the bonds with lengths no shorter than $2r_{eq}$ (r_{eq} is the equilibrium bond length defined by the force field parameters), and label them as "abnormal" bonds. (2) The bond-stretching energy for the "abnormal" bonds is defined as $-k(r - R_{an})^2$, instead of the ordinary form $-k(r - r_{eq})^2$, where R_{an} is an "abnormal bond length" defined for that particular bond. Initially R_{an} is set to the initial bond length of the abnormal bond. (3) R_{an} is reduced by $\Delta R = 0.01$ Å after every MD step. (4) When R_{an} becomes equal or less than r_{eq}, the bond is no longer abnormal, and the atoms are allowed to move under the ordinary bond-stretching potential energy.

Fig. 3 demonstrates how this technique worked. In the initial structure, the benzene ring in the center of the tripod was placed on the plane at $z = 10$ Å, with the center of the benzene ring on the z-axis. The cuboctahedron Au_{147} cluster [16] was then placed at (0,0,0) with one of the 3-fold axis coincide with the z-axis. This caused the central benzene ring to be nearly in van der Waals contact with one of the triangular sides of Au_{147}. The residues in the three legs were placed as follows; the nth residue in the mth leg ($n = 1,\ldots,N$; $m = 1,,2,3$) was located at ($r_0 n^{1/2}\cos\theta$,

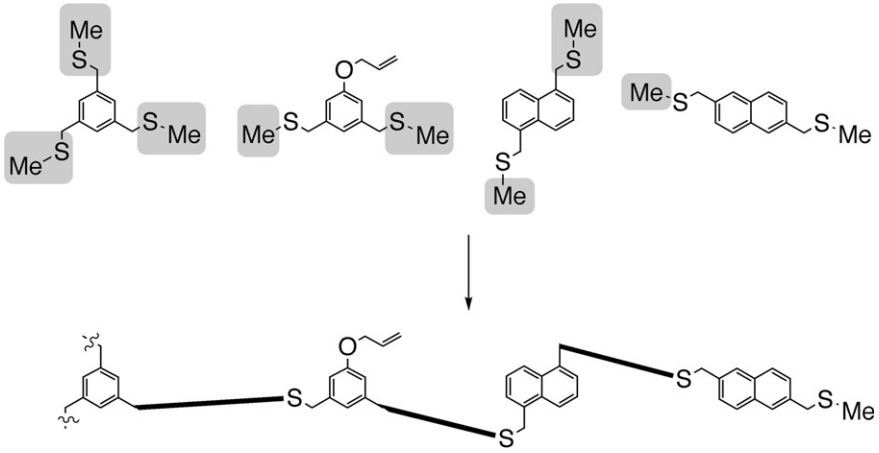

Fig. 2. Automatic construction of the target structure from a sequence "ABC". The bold lines denote the "abnormal" bonds.

$r_0 n^{1/2} \sin\theta$, $r_0(1 - n/2)$) where $\theta = (n\pi/9 - 2m\pi/3)$ and $r_0 =$ 15 Å. As shown in the "top view" of Fig. 3, the residues in one leg were placed along a spiral parallel to the z-axis, and the three legs were placed in a C_3-symmetric orientation. During the first 5000 steps, the abnormal bonds were annealed according to the protocol described above. In addition, the following restrictions were applied: (1) the atoms in the Au_{147} cluster and the central benzene ring were fixed at their initial positions by a harmonic potential with $k = 24$ kcal/mol/Å^2, (2) a central potential $U(r)$ was applied so that the organic atoms were made to approach the cluster surface; $U(r) = 0$ $(r < 12)$, 0.5 $(r - 12)^2$ $(12 \leqslant r < 15)$, 1.5 $(2r - 3)$ $(r \geqslant 15)$, r in Å and U in kcal/mol/Å^2, (3) velocities of all atoms were reinitialized by random values every 50 steps, in order to avoid accumulation of momenta caused by these artificial potentials. After 5000 steps, these artificial potentials were removed and all atoms were allowed to move under ordinary potentials (including our Au–X potentials) at 300 K. As shown in Fig. 3, the molecule smoothly wrapped the Au_{147} cluster during the first 5000 steps, and then started moving on the nanoparticle surface. This protocol is thus useful in finding the stable conformations quickly without human intervention.

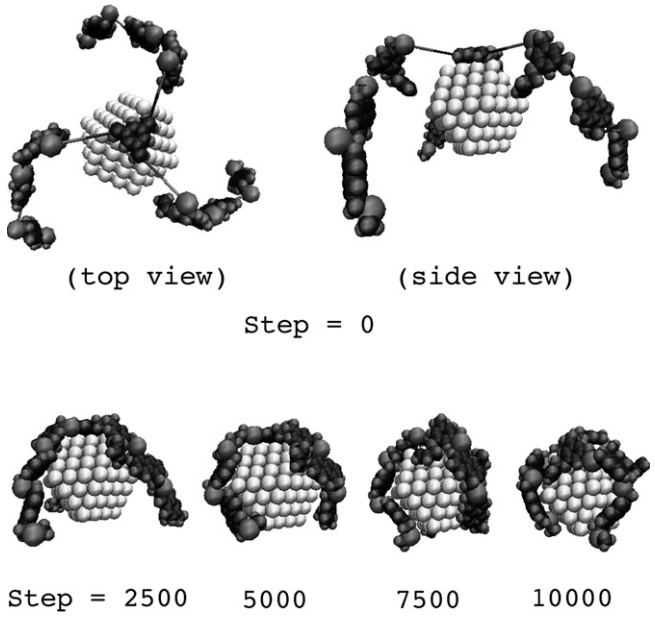

Fig. 3. Selected snapshots of a MD run starting from the automatically generated structure for the sequence "ABC". The gold atoms and organic atoms are shown in white and gray, respectively.

2.4. Search for candidate sequences

We carried out the search for candidate sequences in two stages. In the first (preliminary) stage, a wide range of sequences were calculated for small number of MD steps (5000 steps with restriction and 15,000–20,000 steps without restriction), and only those sequences with lowest energies were selected for the next stage. For $N = 3$ and 4, a full search with all possible combinations was carried out. For $N = 5$ and 6, a search by use of a genetic algorithm [17] (see below) was carried out. In all cases, top 400 sequences were selected for the second (final) stage, where more extensive search for the lowest energy conformations was carried out.

2.5. Application of genetic algorithm

We carried out preliminary search for $N = 5$ and 6 by use of a genetic algorithm as follows: (1) M sequences of length N were randomly prepared. Each sequence is associated with the interaction energy, which was calculated as the lowest value of the sum of Au–X vdW energies in the last MD run. (2) Two "parent" sequences were selected from the M sequences. The probability for a particular sequence i to be selected is proportional to $\exp(-E_i/W)$, where E_i is the associated interaction energy of the sequence i and W is a constant. We set $W = 20$ kcal/mol, which was determined by trial-and-error experimental calculations. (3) Two "child" sequences were generated from the "parent" sequences by a crossing (with 75% probabil-

ity) at one random point followed by mutations of all residues with 30% probability. (4) Repeat (2)–(3) until M different sequences were generated, and perform calculations of these sequences. (5) Select M sequences of lowest interaction energies from the $2M$ sequences of the current and last generations. (6) Repeat (2)–(5) for K times. We used $M = 200$ and $K = 50$ for $N = 5$, and $M = 600$ and $K = 50$ for $N = 6$.

3. Results

3.1. N = 3 and 4

Table 1 lists the top-10 sequences for $N = 3$, and Table 2 lists the statistics of the residues at each position in the sequence. We should note that the ranking of specific sequence may vary because of the fluctuation of the energies due to the random nature of MD simulations. However, we can observe the general trends. The most notable point is that the residues K and L tend to give high scores, whereas the residues A, E, F, and G seldom appear in the high-rank sequences. The top-100 sequences had only two A's, no E, two F's and one G. Particularly, the AAA sequence which we used in the previous study [9] (except for the terminal methylthio groups instead of the tetrahydropyranyloxy groups) did not give a good score; in the preliminary stage its rank was 1314 out of $12^3 = 1728$ sequences.

Table 3 lists the top-10 sequences for $N = 4$, and Table 4 lists the residue statistics. In this case, we omitted residues A, E, F, and G and used only 8 residues. The total number of sequences was thus $8^4 = 4096$. The general trend is very similar to that for $N = 3$. The interaction energy is ca. 50 kcal/mol larger than the $N = 3$ series [18], suggesting more effective protection of the nanoparticle.

Fig. 4 shows the "best-fit" structures for $N = 3$ (LKK) and $N = 4$ (KKDL). Both structures have a substantial portion of the nanoparticle surface left unprotected, although the unprotected portion is reduced in the $N = 4$ complex compared with the $N = 3$ complex.

Table 1
The top-10 sequences for $N = 3$

Rank	Sequence	Energy (kcal/mol)
1	LKK	−305.86
2	KHK	−292.64
3	KLK	−289.37
4	KKL	−286.17
5	LBL	−283.69
6	IKK	−283.14
7	HHK	−282.81
8	KBK	−282.67
9	KLH	−282.64
10	KIK	−282.37
(>400)	AAA	−210.10

Table 2
The residue statistics of the top-100 sequences for $N = 3$

Rank	R^1		R^2		R^3		Total	
1	K	38	K	22	K	32	K	91
2	L	26	L	18	L	19	L	66
3	H	10	C	14	H	12	H	30
4	I	10	B	12	D	11	C	29
5	C	6	I	10	I	9	I	28
6	D	4	D	9	C	9	D	24
7	B	4	H	9	B	4	B	20
8	J	2	J	3	J	2	J	7
9			A	1	A	1	F	2
10			F	1	F	1	A	2
11			G	1			G	1

Table 3
The top-10 sequences for $N = 4$

Rank	Sequence	Energy (kcal/mol)
1	KKDL	−355.94
2	CKKK	−351.28
3	KLDK	−350.29
4	CCLL	−347.48
5	CJKL	−345.86
6	KLKH	−345.18
7	HLKJ	−343.80
8	LBBK	−342.82
9	KHKC	−342.68
10	CKLL	−341.61

3.2. N = 5 and 6

As described in Section 2, we used genetic algorithm in the preliminary search for $N = 5$ and 6. To see whether this algorithm worked as expected, we again included the residues A, E, F, and G and saw how they behaved during

Table 4
The residue statistics of the top-100 sequences for $N = 4$

Rank	R^1		R^2		R^3		R^4		Total	
1	K	48	L	26	K	33	L	26	K	144
2	L	25	K	26	L	20	K	22	L	94
3	D	11	C	13	C	13	D	16	C	35
4	H	7	I	11	H	11	C	12	H	32
5	B	5	B	9	I	9	J	9	D	32
6	I	3	H	6	D	9	B	9	I	28
7	C	1	D	6	B	3	H	3	B	26
8			J	3	J	2	I	3	J	9

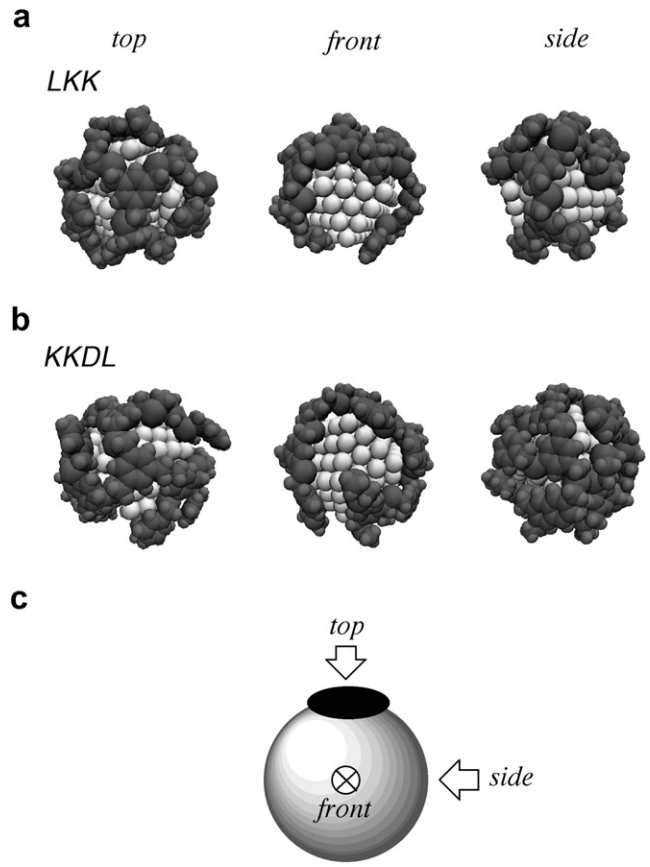

Fig. 4. The lowest energy structures for (a) $N = 3$ and (b) $N = 4$. (c) Description of "top", "front", and "side" views. The dark gray ellipse is the central benzene ring of the protecting molecule.

the "genetic" process for $N = 5$. In each generation, occurrence of each residue was counted over the 200 sequences. The results are shown in Fig. 5. The residues E, F, and G quickly got out within 15 generations while the residues K and L prevailed. The residue A remained, but at substantially low level. After 30 generations change of the population of each residue became gradual, suggesting that the system was approaching the stationary state. Fig. 6 shows the interaction energies (minimum, maximum, and average) in each generation, which also indicates that the energies were approaching the stationary values after 30 generations. These results suggest that the present protocol was useful for quick selection of good candidates.

The top-10 sequences for $N = 5$ and 6 are shown in Tables 5 and 7, and the residue statistics are listed in Tables 6 and 8. The "best-fit" structures are shown in Fig. 7. The surface of the nanoparticle is almost completely covered by the these sequences. Interestingly, the large residues (H, I) are moderately prevalent for $N = 3$ (Table 2), but they become minor for $N = 5$ and 6 and give way to smaller residues like B, C, D, and J (Tables 6 and 8). Another interesting point is that, although K and L (with sulfide side chains) are prevalent in all cases, the best-fit sequence shown for $N = 6$ contained no K and only one L. Careful examination of the structure of HDBBDL revealed presence of three spirals which fill the spherical surface without aid of the side chains (Fig. 8). These structures are the results of competition among residues for the nanoparticle surface area. Our combinatorial calculation automatically took care of the balance of the surface area and the different sizes and shapes of the residues.

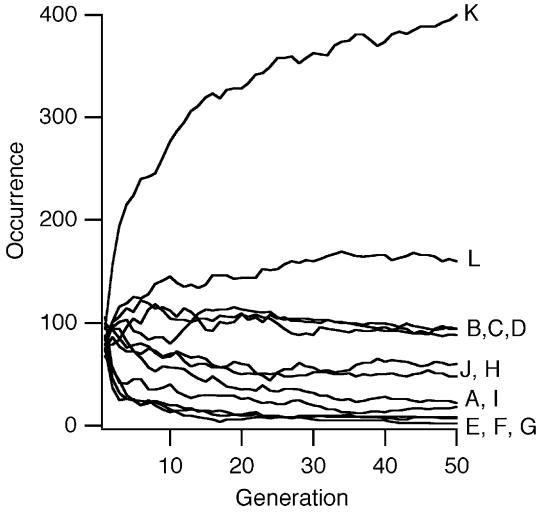

Fig. 5. Population of residues in each generation in genetic calculations for $N = 5$.

3.3. The sequences with a single residue

It is also interesting to examine the results with the sequences with only one residue, like all-A, all-B, etc. Table 9 shows the rank numbers of such sequences for each N. The rank numbers generally show the similar trend with the preference of residues from the residue statistics (Tables 2, 4, 6, and 8), but they did not correspond each other in all

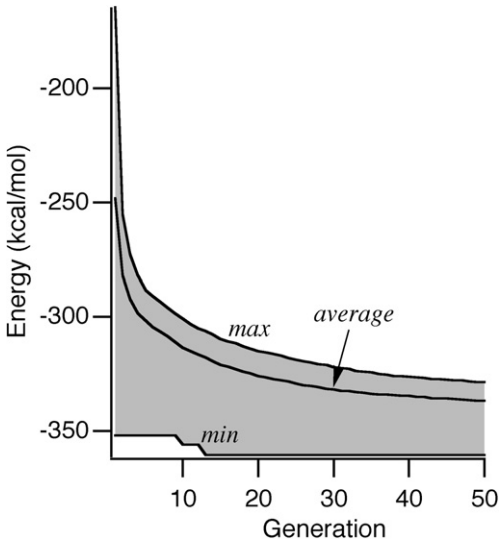

Fig. 6. Distribution of interaction energies in each generation in genetic calculations for $N = 5$.

Table 5
The top-10 sequences for $N = 5$

Rank	Sequence	Energy (kcal/mol)
1	LKLLC	−410.19
2	KBKDJ	−403.11
3	KKLLC	−402.62
4	KKLCK	−399.88
5	LKLLB	−399.38
6	JKDKC	−399.20
7	KCKKL	−398.93
8	KKDKB	−397.40
9	LKKLC	−397.29
10	KCCKK	−394.46

Table 6
The residue statistics of the top-100 sequences for $N = 5$

Rank	R^1		R^2		R^3		R^4		R^5		Total	
1	K	61	K	44	K	59	K	54	C	22	K	234
2	L	18	L	18	L	17	L	19	B	17	L	85
3	B	5	B	12	J	6	B	10	K	16	B	47
4	J	5	C	11	C	5	D	5	D	14	C	43
5	H	4	D	6	D	4	J	4	L	13	D	32
6	D	3	J	5	B	3	C	3	J	10	J	30
7	C	2	H	3	I	2	H	3	I	4	H	15
8	A	1	I	1	H	2	A	1	H	3	I	9
9	I	1			A	1	I	1	A	1	A	4
10					F	1					F	1

Table 7
The top-10 sequences for $N = 6$

Rank	Sequence	Energy (kcal/mol)
1	HDBBDL	−430.51
2	LJLCKB	−427.68
3	JDKKKH	−426.99
4	CLDCDK	−422.26
5	LKDKDC	−421.74
6	LJLCLL	−421.55
7	LCKBLL	−421.54
8	DCDDBK	−419.55
9	ILDLLK	−418.43
10	LDJLBJ	−417.97

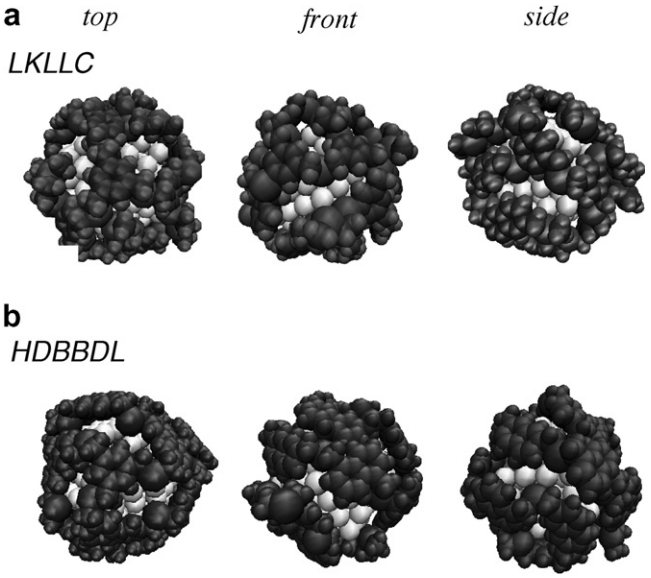

Fig. 7. The lowest energy structures for (a) $N = 5$ and (b) $N = 6$.

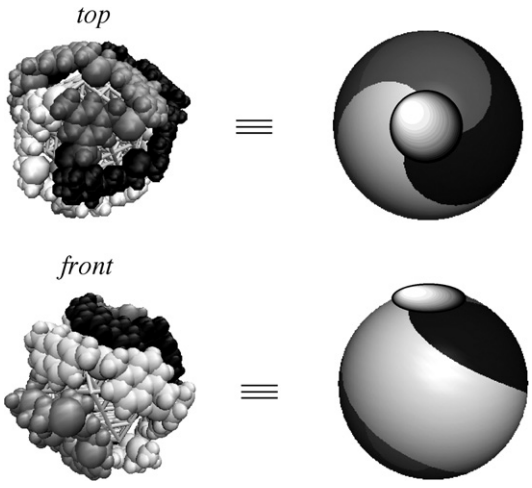

Fig. 8. Alternative views of the lowest energy structure for $N = 6$. The atoms in the three legs are drawn in white, gray, and black. The Au_{147} nanoparticle is shown in wireframe.

Table 8
The residue statistics of the top-100 sequences for $N = 6$

Rank	R^1		R^2		R^3		R^4		R^5		R^6		Total	
1	L	53	C	27	D	26	L	24	K	24	B	22	L	154
2	J	12	L	21	L	17	K	23	D	23	L	18	D	102
3	K	9	D	14	B	17	J	17	L	21	K	18	K	100
4	D	8	B	14	K	17	D	15	B	17	D	16	B	89
5	B	8	J	13	C	14	B	11	C	6	C	8	C	66
6	C	5	K	9	J	8	C	5	J	5	J	8	J	63
7	H	4	A	1	H	1	A	3	I	3	I	4	H	10
8	I	1	I	1			H	2	A	1	H	3	I	9
9											A	2	A	7

cases. Particularly marked deviation was observed for $N = 6$, where the residue L was top in the residue statistics (Table 8) but at the third in Table 9, and the residue C was top in Table 9 but at the fifth in Table 8. Fig. 9 shows the lowest energy structures of the sequences CCCCCC, LLLLLL, and KKKKKK. The structure of CCCCCC is very similar to the "best" sequence HDBBDL (Fig. 8), while the structure of LLLLLL and KKKKKK are more random and some parts of the molecules are sticking out from the nanoparticle surface.

4. Discussion

The problem we are trying to solve is similar to the "pentomino" puzzle [19], where one is supposed to cover a certain area of a checker board with a set of pieces of various shapes. However, the present problem is much more difficult because the area to cover is not planar but spherical, and because the covalent bonds between the "pieces" introduce additional restrictions to the mutual positions and orientations of the neighboring pieces. Moreover, the "pieces" themselves may not be strictly rigid, which can be another source of complication. Molecular simulations can take all these aspects into account, so that they are the methods of choice for this sort of problem.

From the practical point of view, it is useful to know which "residues" are better than other ones. Such information will help us to screen out the "not-so-good" residues and to reduce the number of combinations to try by real synthesis. The residue statistics (Tables 2, 4, 6, and 8) give us such information. The results of the sequences with a single residue (Table 9) also provides a similar information. The residues that generally gave high rank were K and L. This can be attributed to two reasons. One is the presence of extra sulfur atoms that have stronger interaction than carbon atoms. Another is the moderate flexibility of the alkylthio "side chains", which is effective for covering the neighboring area around the main chain. The residue J was less effective, because the methylthio group is too small for this purpose. On the other hand, residues A, E, F, and G did not give good scores. The residues E, F, and G are derivatives of biphenyl, which do not match well to the sur-

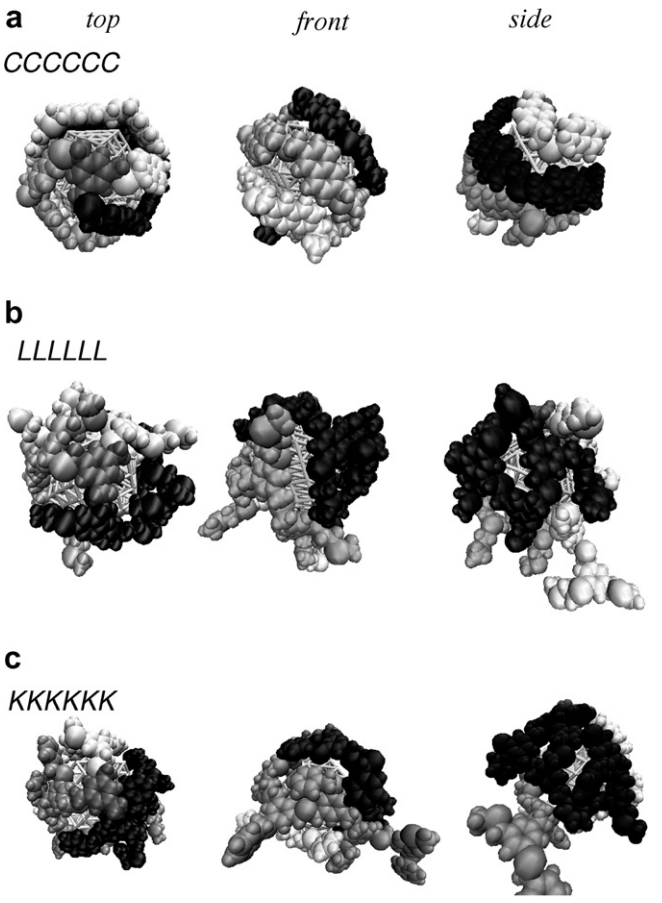

Fig. 9. The lowest energy structures for (a) CCCCCC, (b) LLLLLL, and (c) KKKKKK.

Table 9
The sequences with one residue and their rank[a]

$N = 3$[b]		$N = 4$[b]		$N = 5$[c]		$N = 6$[c]	
LLL	44	KKKK	25	KKKKK[d]	4	CCCCCC	29
KKK	171	LLLL	155	LLLLL	74	KKKKKK	58
DDD	208	HHHH	207	DDDDD	118	LLLLLL	126
HHH	283	DDDD	279	JJJJJ	281	BBBBBB	277
III	289	CCCC	363	HHHHH	376	JJJJJJ	287
CCC	(>400)	JJJJ	380	BBBBB	397	DDDDDD	293
BBB	(>400)	BBBB	(>400)	CCCCC	399	HHHHHH	390
JJJ	(>400)	IIII	(>400)	AAAAA	(>400)	AAAAAA	391
AAA	(>400)	AAAA	(>400)	IIIII	(>400)	IIIIII	(>400)
FFF	(>400)	FFFF	(>400)	FFFFF	(>400)	GGGGGG	(>400)
GGG	(>400)	GGGG	(>400)	EEEEE	(>400)	FFFFFF	(>400)
EEE	(>400)	EEEE	(>400)	GGGGG	(>400)	EEEEEE	(>400)

[a] The rank numbers larger than 400 are undefined, because only 400 sequences were calculated at the final stage.
[b] For $N = 3$ and 4, some of these sequences were not calculated in the final stage because their rank in the preliminary stage was low. In order to estimate the rank for those sequences, they were calculated in the same manner as in the final stage, and the rank numbers were obtained from the merged results.
[c] For $N = 5$ and 6, not all the possible sequences were included in the genetic calculations. The rank numbers of these sequences were estimated as described in footnote b.
[d] The 'KKKKK' sequence does not appear in Table 5, because the genetic calculation did not hit this particular sequence.

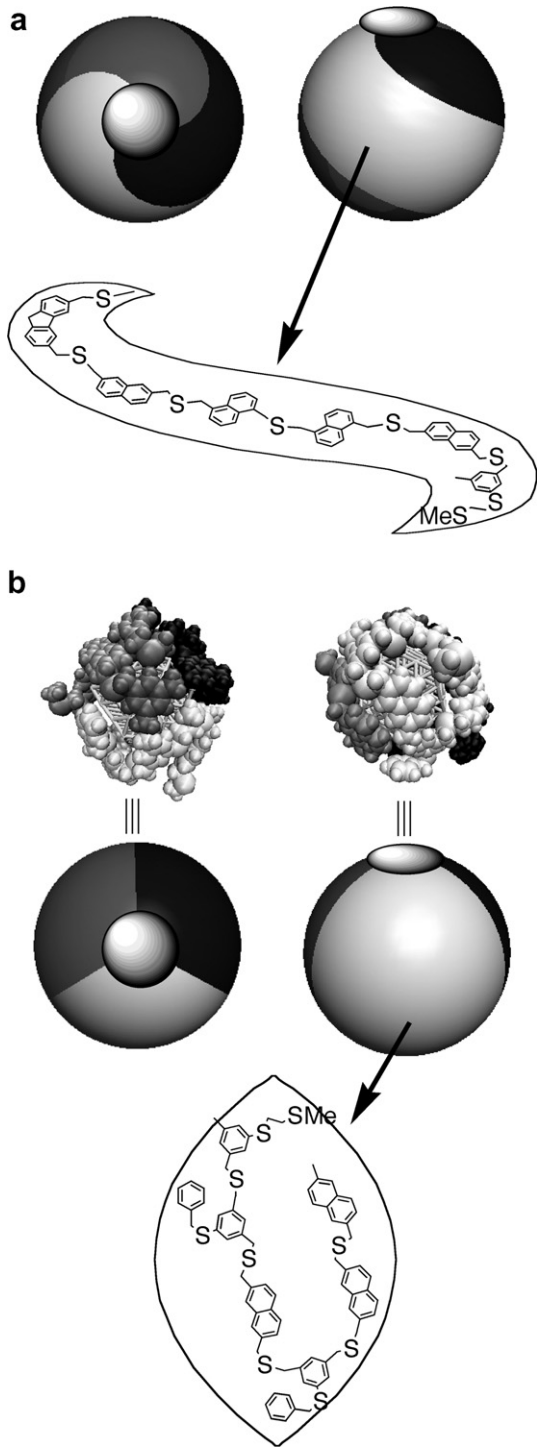

Fig. 10. The surface covering schemes for (a) HDBBDL and (b) LKDKDC. The spherical surface is divided into three areas with approximate 3-fold axis (shown in white, gray and black), and each area is covered with one leg of the tripod molecule. The figures with chemical formula illustrates how each area is covered with the leg.

face of the nanoparticle. The low scores of A is probably due to the small size of the aromatic ring and lack of sulfur atoms in the side chain.

The situation is somewhat special for $N = 6$. We have argued that the residues K and L are good because of their alkylthio side chains, however if the sequences consist of only K or only L, the side chains cannot be accommodated very well because of conflicts between the side chains. The surface coverage is approaching full for $N = 6$, so that the requirement of the shapes of the residues becomes strict (you may recall the pentomino puzzle; when the coverage is low you have many choices, but as the free space decreases the choice becomes narrow quickly). Under such circumstances, it is more important to select proper combinations (or sequences) of residues, rather than to pick a single "good" residue and to use it repeatedly. Apparently, the combinatorial computation is the method of choice for finding such sequences.

In general, it is not straightforward to explain why a particular sequence is better than others, because the interaction energies depend on various factors. However, in some cases the molecular shape alone can account for the efficient coverage. Fig. 10a shows how the tripod molecule with sequence HDBBDL (the "best" sequence in Table 7) covers the nanoparticle surface. As shown in Fig. 8, the lowest-energy structure has approximately 3-fold symmetry. Each leg covers 1/3 of the spherical surface in a helical manner. The 1/3 part of the sphere has a characteristic shape, with steep curves at both ends and a flat area in between. The residues H and L fit the curvy ends, and the sequence DBBD fits the flat area. The arrangement of these residues match their shapes very well. Another clear example is the sequence LKDKDC (Fig. 10b; rank 5 in Table 7). The lowest-energy structure for this sequence also had approximate 3-fold symmetry, but the area occupied by each leg was not helical but straight, i.e. the areas are roughly separated by the longitude lines. In this case, each leg should make a turn to cover the area, because the area is too wide and too short to accommodate one leg in its stretched form. The sequence DKD provides such a turn. Admittedly, these symmetric structures were rather exceptional, and most other sequences gave more random structures. Nevertheless, it is insightful that, at least in some cases, very reasonable structures can be formed from apparently featureless sequences.

5. Conclusion

We propose here a computational method for designing protecting molecules for metal nanoparticles. Although the computations include a number of crude approximations, the results are predictive and useful. In combination with synthetic works, the present method will provide new insights about soft nanomaterials consisting of nanoparticles and organic molecules.

Acknowledgements

The author thanks Dr. Suguru Maki, Dr. Takayuki Nagasawa and Prof. Takuji Ogawa (IMS) for helpful discussion, and Research Center for Computational Science of Okazaki Research Facilities (NINS) for the use of the

SGI2800 computer. The author also thanks one reviewer for insightful comments. This work was supported by a Grant-in-aid for Scientific Research in Priority Area, "Reaction Control of Dynamic Complexes" (No. 16033262) of the Ministry of Education, Culture, Sports, Science and Technology (MEXT), Japan.

Appendix A. Supplementary data

Supplementary data associated with this article can be found, in the online version, at doi:10.1016/j.jorganchem.2006.05.058.

References

[1] (a) G. Schmid (Ed.), Nanoparticles, Wiley-VCH, Weinheim, 2004;
(b) L.M. Liz-Marzan, P.V. Kamat (Eds.), Nanoscale Materials, Kluwer, 2003.
[2] (a) Y. Xue, M.A. Ratner, Phys. Rev. B 70 (2004) 155408;
(b) J. Wu, L. Ma, Y. Yang, Phys. Rev. B 69 (2004) 115321;
(c) D. Lee, R.L. Donkers, J.M. DeSimone, R.W. Murray, J. Am. Chem. Soc. 125 (2003) 1182;
(d) H.-G. Boyen, G. Kastle, F. Weigl, P. Ziemann, G. Schmid, M.G. Garnier, P. Oelhafen, Phys. Rev. Lett. 87 (2001) 276401;
(e) C.A. Berven, L. Clark, J.L. Mooster, M.N. Wybourne, J.E. Hutchison, Adv. Mater. 13 (2001) 109;
(f) F. Remacle, R.D. Levine, ChemPhysChem 2 (2001) 20.
[3] (a) E. Hutter, J.H. Fendler, Adv. Mater. 16 (2004) 1685;
(b) F. Stellacci, C.A. Bauer, T. Meyer-Friedrichsen, W. Wenseleers, S.R. Marder, J.W. Perry, J. Am. Chem. Soc. 125 (2003) 328;
(c) P.V. Kamat, J. Phys. Chem. B 106 (2002) 7729;
(d) L. Xu, W. Zhou, M.E. Kozlov, I.I. Khayrullin, I. Udod, A.A. Zakhidov, R.H. Baughman, J.B. Wiley, J. Am. Chem. Soc. 123 (2001) 763;
(e) S. De, A. Pal, T. Pal, Langmuir 16 (2000) 6855.
[4] (a) R. Narayanan, M.A. El-Sayed, J. Phys. Chem. B 109 (2005) 12663;
(b) J.K. Edwards, B. Solsona, P. Landon, A.F. Carley, A. Herzing, M. Watanabe, C.J. Kiely, G.J. Hutchings, J. Mater. Chem. 15 (2005) 4595;
(c) J. Huang, Z. Liu, C. He, L.M. Gan, J. Phys. Chem. B 109 (2005) 16644;
(d) L.S. Ott, M.L. Cline, M. Deetlefs, K.R. Seddon, R.G. Finke, J. Am. Chem. Soc. 127 (2005) 5758;
(e) K. Okamoto, R. Akiyama, H. Yoshida, T. Yoshida, S. Kobayashi, J. Am. Chem. Soc. 127 (2005) 2125;
(f) R.W.J. Scott, O.M. Wilson, S.-K. Oh, E.A. Kenik, R.M. Crooks, J. Am. Chem. Soc. 126 (2004) 15583;
(g) Y. Na, S. Park, S.B. Han, H. Han, S. Ko, S. Chang, J. Am. Chem. Soc. 126 (2004) 250;
(h) S. Fukuzumi, Y. Endo, Y. Kashiwagi, Y. Araki, O. Ito, H. Imahori, J. Phys. Chem. B 107 (2003) 11979;
(i) K.-M. Choi, T. Mizugaki, K. Ebitani, K. Kaneda, Chem. Lett. 32 (2003) 180;
(j) N. Toshima, in Ref. [1b], pp. 79–96;
(k) M. Haruta (Ed.), Studies in Surface Science and Catalysis, vol. 145, Elsevier, 2003.
[5] M. Brust, M. Walker, D. Bethell, D.J. Schiffrin, R. Whyman, Chem. Commun. (1994) 801.
[6] (a) U. Drechsler, B. Erdogan, V.M. Rotello, Chem. Eur. J. 10 (2004) 5570;
(b) D. Roy, J. Fendler, Adv. Mater. 16 (2004) 479;
(c) T. Pradeep, N. Sandhyarani, Pure Appl. Chem. 74 (2002) 1593;
(d) A.C. Templeton, W.P. Wuelfing, R.W. Murray, Acc. Chem. Res. 33 (2000) 27.
[7] (a) F. Callari, S. Petralia, S. Sortine, Chem. Commun. (2006) 1009;
(b) B. Su, H.H. Girault, J. Phys. Chem. B 109 (2005) 23925;
(c) A.R. Rothrock, R.L. Donkers, M.H. Schoenfisch, J. Am. Chem. Soc. 127 (2005) 9362;
(d) A. Arduini, D. Demuru, A. Pochini, A. Secchi, Chem. Commun. (2005) 645;
(e) N.O. Fischer, R. Paulini, U. Drechsler, V.M. Rotello, Chem. Commun. (2004) 2866;
(f) T.-Y. Dong, H.-W. Shih, L.-S. Chang, Langmuir 20 (2004) 9340;
(g) Y. Negishi, T. Tsukuda, Chem. Phys. Lett. 383 (2004) 161;
(h) A.J. Kell, C.C. Montcalm, M.S. Workentin, Can. J. Chem. 81 (2003) 484;
(i) T. Gu, T. Ye, J.D. Simon, J.K. Whitesell, M.A. Fox, J. Phys. Chem. B 107 (2003) 1765.
[8] (a) C.M. Kraemer-Pecore, A.M. Wollacott, J.R. Desjarlais, Curr. Opin. Chem. Biol. 5 (2001) 690;
(b) J. Zeng, T. Nheu, A. Zorzet, B. Catimel, E. Nice, H. Maruta, A.W. Burgess, H.R. Treutlein, Protein Eng. 14 (2001) 39;
(c) F.H. Arnold, Nature (London) 409 (2001) 253;
(d) K. Suzuki, S. Takami, M. Kubo, A. Miyamoto, Yuki Gosei Kagaku Kyokaishi (J. Synth. Org. Chem. Jpn.) 60 (2002) 488;
(e) A. Cheng, D.J. Diller, S.L. Dixon, W.J. Egan, G. Lauri, K.M. Merz Jr., J. Comput. Chem. 23 (2002) 172.
[9] Y. Hosokawa, S. Maki, T. Nagata, Bull. Chem. Soc. Jpn. 78 (2005) 1773.
[10] D.A. Case, D.A. Pearlman, J.W. Caldwell, T.E. Cheatham III, J. Wang, W.S. Ross, C.L. Simmerling, T.A. Darden, K.M. Merz, R.V. Stanton, A.L. Cheng, J.J. Vincent, M. Crowley, V. Tsui, H. Gohlke, R.J. Radmer, Y. Duan, J. Pitera, I. Massova, G.L. Seibel, U.C. Singh, P.K. Weiner, P.A. Kollman, Amber 7, University of California, San Francisco, 2002.
[11] (a) L. Kal, R. Skeel, M. Bhandarkar, R. Brunner, A. Gursoy, N. Krawetz, J. Phillips, A. Shinozaki, K. Varadarajan, K. Schulten, J. Comput. Phys. 151 (1999) 283;
(b) http://www.ks.uiuc.edu/Research/namd/.
[12] Y. Kikuzawa, T. Nagata, Bull. Chem. Soc. Jpn. 77 (2004) 993.
[13] (a) W. Humphrey, A. Dalke, K. Schulten, J. Mol. Graph. 14 (1996) 33;
(b) http://www.ks.uiuc.edu/Research/vmd/.
[14] C.I. Bayly, P. Cieplak, W.D. Cornell, P.A. Kollman, J. Phys. Chem. 97 (1993) 10269.
[15] M.W. Schmidt, K.K. Baldridge, J.A. Boatz, S.T. Elbert, M.S. Gordon, J.H. Jensen, S. Koseki, N. Matsunaga, K.A. Nguyen, S.J. Su, T.L. Windus, M. Dupuis, J.A. Montgomery, J. Comput. Chem. 14 (1993) 1347.
[16] (a) In the present study the shape of the nanoparticle is fixed to an idealized cuboctahedron. Although it is questionable that nanoparticles of this size have such fixed conformations (see the following references), consideration of the dynamic feature of the nanoparticle causes another complication that is unnecessary at this stage;
(b) O.D. Haeberlen, S.-C. Chung, M. Stener, N. Roesch, J. Chem. Phys. 106 (1997) 5189.
[17] (a) B. Hartke, J. Phys. Chem. 97 (1993) 9973;
(b) G. Boehm, Biophys. Chem. 59 (1996) 1;
(c) J. Apstolakis, A. Caflisch, Comb. Chem. High Throughput Screening 2 (1999) 91.
[18] We will not discuss the absolute values of the interaction energies, because the force-field parameters include too many assumptions for quantitative arguments to be valid. Instead, we will treat these numbers as if they were in "arbitrary units," and limit our discussion to qualitative aspects.
[19] S.W. Golomb, Amer. Math. Mon. 61 (1954) 675.